

# Modelling of Electrostatics in Nanofluidic Channels

Pankaj Asija<sup>1</sup> and Subhra Datta<sup>2,\*</sup>

<sup>1</sup>ONGC Ltd., Surat, Gujarat, India

<sup>2</sup>Department of Mechanical Engineering, IIT Delhi, India

## ABSTRACT

The equilibrium interaction between the processes of charge formation on the surface of a nanochannel and ionic distribution within the confined electrolyte is studied for situations where electric-double-layer (EDL) are of size comparable to the nanochannel cross-dimension and the mean-field surface electrostatic potential is comparable to or larger than the thermal energy per unit charge of an ion. The effects of channel size, pH, ionic composition and the compact region of the electric double layer are investigated. The results can be used for understanding electrokinetic phenomena involving current conduction and fluid flow in nanochannels, as demonstrated through a comparison of the theoretical results with measured electrical conductance data.

## 1. INTRODUCTION

When a solid surface comes in contact with water or an aqueous solution, it forms a surface charge which in turn results in a near-surface crowding of predominantly oppositely charged ions from the solution forming an electrical double layer (EDL) [1]. The Guoy-Chapman-Stern-Grahame model [1] posits the EDL to be composed of a near-surface compact zone termed Stern layer followed by a larger diffuse zone further away. The EDL can be taken advantage of to realize electrokinetic phenomena such as electro-osmosis, streaming current and electrophoresis through the external imposition of forces and/or motion. While studying electrokinetic phenomena, it is common to assume in the electrostatic model that the effect of formation of charges on the electrical double layers can be imposed through either a (i) specified surface potential, or (ii) a specified surface charge density.

A large fraction of historical studies (see *e.g.* [2], [3],[4]) and even recent studies (see for example, [5]) requiring the solution of the Poisson-Boltzmann equation employ boundary condition (i). The specified surface charge boundary condition (itemized above as (ii)) has gained more recent attention in nanofluidics, because of its purported less sensitivity to solution ionic concentration and evidence from studies on current conduction in nanochannels [6],[7].

It has been long realized (see *e.g.* [8]) that neither specifying surface charge nor specifying surface potential on a wall is an adequate representation of reality. In fact, both these boundary condition ignore the charge formation process on the wall. However, a majority of such studies appreciating this fact [9], [10], [11], [12] and the references therein are theoretically formulated to study a single ionizing surface in contact with an electrolyte. In the context of microfluidic applications, taking into account the electrostatic screening effect at typical ionic strengths (of the order of 0.01–100 mM), it can be inferred that these models will be limited to systems employing microchannels rather than nanochannels. With the progressive reduction of experimentally achievable scales to the nanometer level [13], it is essential to further generalize the charge formation and electrical double layer (EDL) models in these works.

Developing a “surface ionization model” and understanding the effect of model input parameters arising from nanochannel geometry and electrolyte composition as well as the assumed compact-diffuse structure of the EDL will be a principal thrust of this study. Further, the electrostatic model developed will be employed to understand experimental data from [7] on external electric field driven charge transport in through nanochannels. For the sake of generality, the Debye-Huckel linearization of

---

\*Corresponding author: subhra.datta@mech.iitd.ac.in

the electrostatic model which is strictly applicable only to weakly charged surfaces [14] and the isolated surface approximation[15] via the Grahame equation[1] which can be too restrictive for nanofluidic situations are both avoided in this study. Two other studies, in with the charge formation and EDL models are formulated in a form applicable to nanochannels are [6] and [16].

The development of the surface ionization model and a semi-analytical efficient grid-free procedure to solve the same is discussed in detail. At no stage of the electrostatic and the electrokinetic model, numerical discretization (as in[17],[18], [19] ) and/or numerical differentiation (as in[6]) is resorted to; this feature of the model leads to quick and accurate predictions. Although, the authors of [16] model the same physical processes at equilibrium as in the current work, the electrostatic model is not applied to study any non-equilibrium phenomenon, as done in the current work through comparison with experimental data on current conduction in nanochannels.

The following two sections of this article discuss the theoretical model and its semi-analytical solution procedure. The effects of various input parameters are studied and comparison with an electrokinetic experiment in nanochannel is presented in the section titled “Results and Discussion”. Important conclusions and the scope for future work are identified in the final section of this article.

## 2. THEORETICAL FORMULATION

Consider two infinitely long and wide solid surfaces separated by a distance  $2h$  in a solution containing a completely dissociating binary electrolyte of concentration  $n_{\infty}$ . A model to predict the surface charge acquired by the walls of this nanochannel will be coupled in this section to the model for predicting ionic charge distribution in the confined solution. This approach will obviate the necessity to provide surface charge density [6-7] and/or zeta potential [2-5] as inputs to models to study electrokinetic phenomena and/or electrostatic interactions. The physical process and the corresponding mathematical representations are discussed in detail below.

When the surface of a siliceous materials such as glass, quartz, fused silica (typical forms used in microfluidics) comes in contact with water or an aqueous solution, it is known to acquire a negative surface charge density, primarily through the dissociation of the terminal silanol (SiOH) groups, a process which releases a proton from the surface to the solution and forms a negatively charged group on the surface. The degree of dissociation and thus the surface charge density is determined from the equilibrium in the presence of the electrical double layer between the ions formed at the glass surface and the free ions in the bulk electrolyte.

In the following discussion, it has been assumed that surface acquire positive for the sake of simplicity. The hypothetical groups  $B^-$  and  $A^+$  discussed below can, therefore, be considered oppositely charged analogues of the dissociated hydrogen ion and the ionized silanol group, respectively. Extension of the results obtained to a negatively charged surface is trivial. The mechanism by which glass and silica surface acquire a charge in contact with water is the dissociation of silanol groups and can be represented by



Within this model the charge on the solid is regarded as localized entirely on the surface and arising from a concentration of dissociated head groups (*e.g.* silanol in case of silica), giving rise to the surface charge density

$$\sigma = +e\Gamma_{A^+} \quad (2)$$

However, only a fraction of the total concentration of chargeable sites dissociate. Therefore,

$$\Gamma = \Gamma_{A^+} + \Gamma_{AB} \quad (3)$$

Here,  $\Gamma$  is total site density and it is assumed to be constant ( $\Gamma = 8 \text{ nm}^{-2}$ ) in this model. In dilute solutions, the dissociation process in eqn. (1) is characterized by an equilibrium constant  $K$  defined by

$$\frac{[B^-]_0 \Gamma_{A^+}}{\Gamma_{AB}} = 10^{-pK} \quad (4)$$

The dissociation constant is estimated to be in the range [9], [11], [12], [16], [20]  $pK = -\log_{10} K = 5.8-7.5$ . Henceforth, the straight bracket indicates volumetric concentration expressed in moles per liter and the subscript “0” indicates “as evaluated on the ionizing surface”. Due to Boltzmann equilibrium

$$[B^-]_0 = [B^-]_b \exp\left(\frac{e\varphi_0}{k_B T}\right) \quad (5)$$

Here,  $[B^-]_b = 10^{-pH}$  mole/liter is the bulk concentration of the species  $B^-$  and  $k_B T$  denotes the thermal energy. Here, the bulk concentration should be interpreted to be the concentration of the salt that prevails in reservoirs of dimensions much larger than the nanochannel that are connected to the ends of the nanochannel. In this situation, eqn. (5) is an expression of electrochemical equilibrium [21], [22], [23] between the reservoir and the channel interior. A different model for overlapped EDLs in an infinitely long thin channel which rather than using the equilibrium criteria given by eqn. (5) involves conserving the mass of each EDL ionic species assuming one-dimensional diffusion and migration perpendicular to the walls after the formation of surface charge, also appears in the literature [24], [25]. It has been suggested [26] on the basis of simulation of a perturbed electrical double layer in a reservoir-connected closed system using the transient Nernst-Planck equations with convection that that models discussed in [24], [25] is representative of intermediate quasi-equilibrium state reached after the typical cross-diffusion time, whereas eqn. (5) represents the long-time equilibrium reached after the typical axial diffusion/convection times. For studying certain kinds of electrokinetic phenomena which involve applied forces such as electric field and pressure-gradients, Eqn. (5) has been classically used in the literature [27]; this usage (also adopted in the current work) can be interpreted in the sense of small/no departure from the layering of ions perpendicular to the walls of a long channel which is reached after the long-time-equilibrium discussed above.

Eqns. (1)-(5) may be combined to read

$$\exp\left(\frac{e\varphi_0}{k_B T}\right) = 10^{-pK+pH} \times \frac{(\Gamma e - \sigma)}{\sigma} \quad (6)$$

where  $pH = -\log_{10}[B^-]_b$ . The diffuse layer of counterions is assumed to be separated from the ionizing surface by a thin Stern layer across which the electrostatic potential drops linearly from the value  $\varphi_0$  to a value  $\varphi_d$  called the diffuse layer potential [9]. This potential drop is characterized by the Stern layer capacitance ( $C$ ) defined by  $C = \frac{\sigma}{\varphi_0 - \varphi_d}$ . Using this definition and introducing dimensionless variables of the form  $\varphi^* = e\varphi/(k_B T)$ , eqns. (6) and (7) can be combined to

$$\exp(\varphi_d^*) = 10^{-pK+pH} \times \frac{(\Gamma e - \sigma)}{\sigma} \times \exp\left(-\frac{\sigma e}{Ck_B T}\right) \quad (7)$$

Under consideration is the region away from the reservoir channel interface, where the layering of ions occurs perpendicular to the straight walls. Integration of the Poisson-Boltzmann equation in the gap  $2h$  between two parallel plates for a symmetric binary 1:1 electrolyte leads to the forms (as derived in [28]) leads to

$$\varphi_d^* = \varphi_c^* - 2 \ln[cd(\frac{h}{2\lambda\sqrt{k}}, k)] \quad (8)$$

$$\frac{d\varphi^*}{dy^*} = \frac{sn\left(\frac{y^*}{2\sqrt{k}}, k\right)}{cn\left(\frac{y^*}{2\sqrt{k}}, k\right) \times dn\left(\frac{y^*}{2\sqrt{k}}, k\right)} \left(\frac{1}{\sqrt{k}} - k\sqrt{k}\right) \quad (9)$$

where  $\varphi_c$  is the electric potential at the centerline of the channel,  $k = \exp(-\phi_c^*)$  and the dimensionless variable  $y^* = y/\lambda$  is the ratio of the distance from channel symmetry axis to the Debye length  $\lambda$  in the electrolyte.

Here,  $sn(p, q)$ ,  $cn(p, q)$ ,  $dn(p, q)$  and  $cd(p, q)$  are Jacobi elliptic functions with argument  $p$  and modulus  $q$ [29]. Eqn. (8) can be rearranged into

$$k = \frac{1}{\exp(\varphi_d^*) \times [cd(\frac{h}{2\lambda\sqrt{k}}, k)]^2} \quad (9)$$

Using  $\exp(\varphi_d^*)$  from eqn. (7)

$$k = \frac{10^{(pK-pH)}}{cd^2} \times \frac{\sigma}{(\Gamma e - \sigma)} \times \exp\left(\frac{\sigma e}{Ck_B T}\right) \quad (10)$$

where  $cd$  is an abbreviation for the term within straight brackets in eqn. (9). In terms of the dimensionless surface charge density,  $\sigma^* = \frac{\sigma e \lambda}{\epsilon k_B T}$  and  $\Gamma^* = \frac{\Gamma e^2 \lambda}{\epsilon k_B T}$ , eqn. (10) can be written as

$$k = \frac{10^{(pK-pH)}}{cd^2} \times \frac{\sigma^*}{(\Gamma^* - \sigma^*)} \times \exp\left(\frac{\epsilon \sigma^*}{C \lambda}\right) \quad (11)$$

The surface charge density also satisfies the boundary condition  $\sigma^* = d\varphi^*/dy^*|_{y=h/\lambda}$  which can be used in eqn. (9) leading to

$$\sigma^* = \frac{sn\left(\frac{h}{2\lambda\sqrt{k}}, k\right)}{cn\left(\frac{h}{2\lambda\sqrt{k}}, k\right) \times dn\left(\frac{h}{2\lambda\sqrt{k}}, k\right)} \left(\frac{1}{\sqrt{k}} - k\sqrt{k}\right) \quad (12)$$

Solution of eqns. (11) and (12) completely specifies the electric potential distribution although not tractable analytically. It can be noted here that the Stern plane will be assumed to be coincident with the shear plane in this work and therefore, the zeta potential  $\zeta = \varphi_d$ .

### 3. SOLUTION PROCEDURE

A fixed point iteration technique with current iteration number denoted by  $N$  was based on eqns. (11) and (12) via the following successive evaluations:

$$\sigma_N^* = \frac{\operatorname{sn}\left(\frac{h}{2\lambda\sqrt{k_N}}, k_N\right)}{\operatorname{cn}\left(\frac{h}{2\lambda\sqrt{k_N}}, k_N\right) \times \operatorname{dn}\left(\frac{h}{2\lambda\sqrt{k_N}}, k_N\right)} \left( \frac{1}{\sqrt{k_N}} - k_N \sqrt{k_N} \right) \quad (13)$$

$$k_{N+1} = \frac{10^{(pK-pH)}}{cd^2} \times \frac{\sigma_N^*}{\Gamma_{ND} - \sigma_N^*} \times e^{\left(\frac{\epsilon\sigma_N^*}{C\lambda}\right)} \quad (14)$$

A relaxation factor ( $0 < r < 1$ ) was used to under-relax the above iteration scheme. The convergence criteria used was  $\left| \frac{k^{N+1} - k^N}{k^N} \right| \leq 10^{-11}$ .

### 4. RESULTS AND DISCUSSION

The discussion of results in this section will be mainly in reference to the silica surface, although the mathematical model has been developed for its oppositely charged analogue. The variables in displayed figures will also adhere to the sign of charges adopted in the mathematical model. To relate the equations discussed beforehand and the figures to be presented below to the silica surface, the transformation mathematically required is simply inserting a negative sign before all calculated potentials and charges. However, for brevity, this will not be resorted to explicitly; instead reference will be made to *magnitudes* of quantities such as zeta potential and surface charge density.

At the onset of this section, a convenient interpretation of the theoretical model developed in the previous section can be noted. Rearranging eqn. (10)

$$\sigma = \Gamma e \left\{ \frac{10^{-pK}}{10^{-pH} \exp\left[\frac{e}{k_B T} \left( \zeta(\sigma) + \frac{\sigma}{C} \right)\right] + 10^{-pK}} \right\} \quad (15)$$

The expression in curly brackets can be interpreted in the context of silica (with the transformation discussed above) to be the fraction of the total number of silanol sites on the surface that dissociates to form the surface charge. The first term in the denominator of this expression can be considered to be the (volumetric) concentration of  $H^+$  ions *on the surface* where the silanol groups reside. This term is a product of two factors, the factor  $10^{-pH}$  is the bulk (reservoir) concentration of  $H^+$  ions and the exponential quantity multiplying this factor is an enhancement/depletion originating from the Boltzmann equilibrium of  $H^+$  ions. The latter factor is dependent on the electric potential (the term within brackets inside the exponential) on the surface of adsorption.

Following inference of the effect of certain input parameters can be drawn based on eqn. (15) and will not be investigated further. A large site density will give rise to a large surface charge density and a large  $pK$  (weakly dissociating surface) will lead to a small surface charge, as expected on physical grounds.

However, it can be noted that eqn. (15) is not an explicit expression for the surface charge density, since the zeta potential depends on surface charge as indicated by the function notation used and that the second term inside the bracket within the exponential signifies a change in potential in the Stern layer which is proportional to the surface charge.

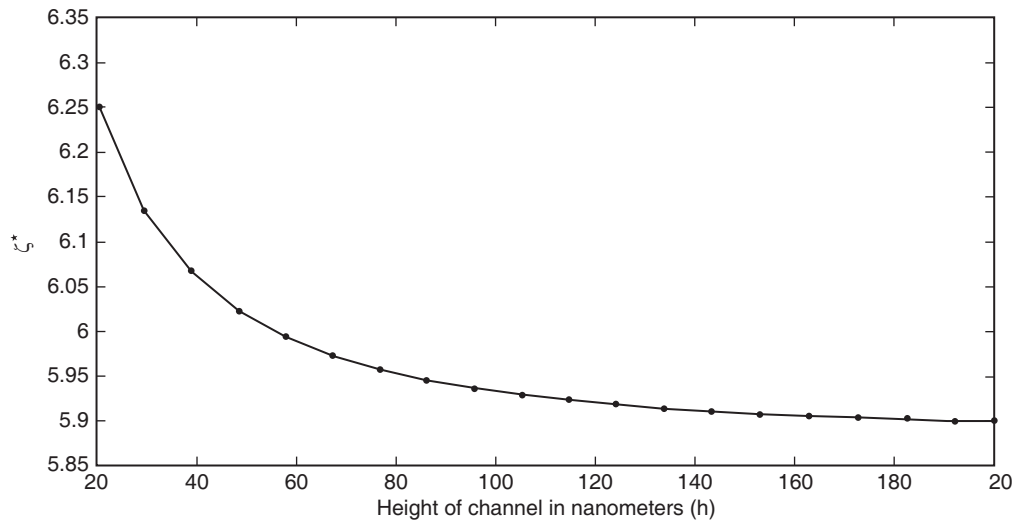


Figure 1. The dependence of surface potential on height of channel for input parameters:  $\rho K = 7.5$ ,  $C = 2.9 \text{ F/m}^2$ ,  $\Gamma = 8/\text{nm}^2$ ,  $\text{pH} = 7$ ,  $n_\infty = 0.001 \text{ mM}$

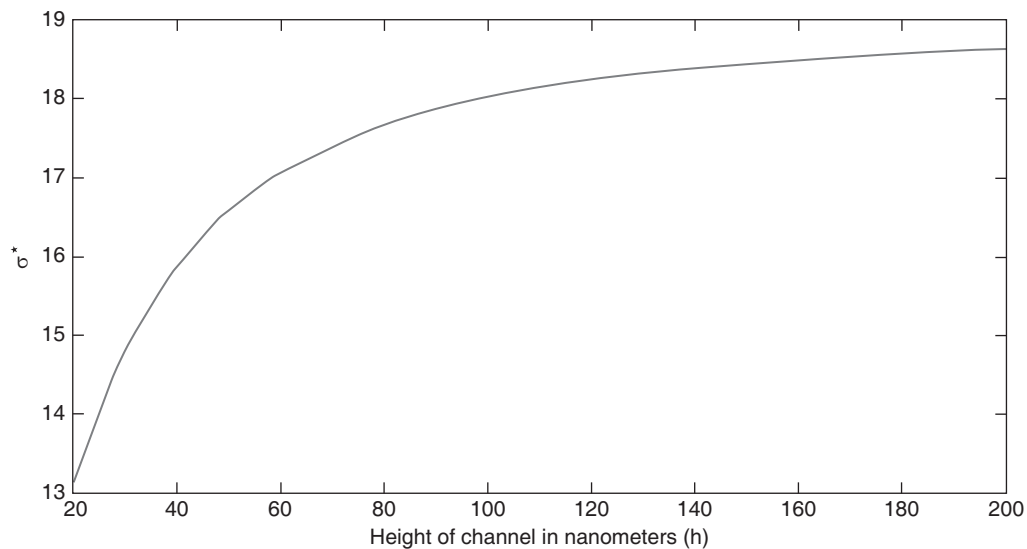


Figure 2. The dependence of surface charge density on height of channel for input parameters  $\rho K = 7.5$ ,  $C = 2.9 \text{ F/m}^2$ ,  $\Gamma = 8/\text{nm}^2$ ,  $\text{pH} = 7$ ,  $n_\infty = 0.001 \text{ mM}$

Certain conclusions made in the study of the effect of different parameters like pH, Stern layer capacitance can be qualitatively rationalized in terms of eqn. (15), while temporarily ignoring the implicitness discussed above, although in the remainder of this study, this equation will not be explicitly referenced for explanations. In the following discussion, the effects of various input parameters of the model on the surface charge density and zeta potential, no qualitative deviations were noticed between the “true picture” obtained by solving the full model with the picture inferred from eqn. (15) with the above assumption, though such a possibility exists mathematically (*e.g.* for the effect of Stern layer capacitance) if the implicit dependences are strong.

Figure 1 shows the variation of dimensionless surface zeta potential ( $\zeta^*$ ) as a function of height of channel ( $h$ ). It can be observed from Figure 1 that the dimensionless surface zeta potential  $\zeta^*$  is higher

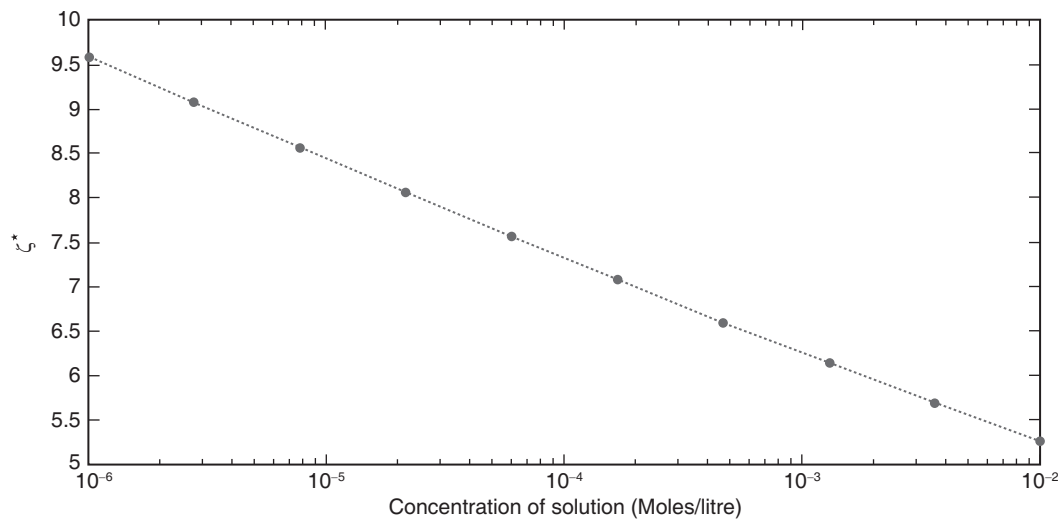


Figure 3. The dependence of surface potential on concentration of solution for the following input parameters:  $pK=7.5$ ,  $C=2.9 \text{ F/m}^2$ ,  $h = 20 \text{ nm}$ ,  $\Gamma = 8/\text{nm}^2$ ,  $pH = 7$

for a narrow channel. This can be explained as for a constant surface charge density condition the number density of counter ions increases as the channel thickness is decreased and a higher surface potential will be required to populate the channel with a larger density of counter-ions.

Figure 2 shows the variation of dimensionless surface charge density  $\sigma^*$  as a function of height of channel ( $h$ ). It can be observed from Figure 2 that  $\sigma^*$  is lower for a narrow channel. This fact can be understood since the narrowness of channel yields high values of electric potential within the channel. The higher potential leads to a higher availability of  $\text{H}^+$  ions (according to Boltzmann equilibrium) on the surface which lowers the degree of dissociation of silica surface (to preserve chemical equilibrium). The reduced dissociation at the silica surface leads to decrease in surface charge. From Figures (1) and 2, it can be concluded that, unlike in microchannels, the degree of completion of the charge forming chemical process on the walls of a nanochannel is dependent on the channel size.

Figure 3 shows the variation of dimensionless surface zeta potential ( $\zeta^*$ ) as a function of concentration of solution. It can be observed from the Figure 3 that the dimensionless surface zeta potential ( $\zeta^*$ ) is higher for a lower concentration. This can be explained as for a higher concentration reservoir condition a larger number of counter ions is present in the EDL. Hence, with this larger number of counter-ions per unit volume, lower electrical potential energy levels within the nanochannel are sufficient to balance the surface charge. This leads to a lower surface potential.

Figure 4 shows the variation of dimensionless surface charge density  $\sigma^*h/\lambda$  as a function of concentration of solution. It can be observed from the Figure 4 that the dimensionless surface charge density is higher for a higher concentration. This can be explained based on the conclusion from the previous figure that the zeta potential decreases with increasing concentration. This means that less  $\text{H}^+$  ions are available on the ionizing surface, which promotes increased dissociation (to preserve chemical equilibrium), which in turn leads to a higher surface charge densities.

Figure (5) shows the variation of dimensionless surface charge density ( $\sigma^*$ ) as a function of pH of the solution. It can be observed from the Figure (5) that  $\sigma^*$  increases as the pH of the solution increases. This can be explained as for a higher pH value, the availability of the  $\text{H}^+$  ion in the solution is less which leads to more dissociation of the silica surface, to preserve chemical equilibrium. Hence, more dissociation of the silica surface causes the higher surface charge.

Figure 6 shows the variation of dimensionless surface zeta potential ( $\zeta^*$ ) as a function of pH of the solution. It can be observed from figure that  $\zeta^*$  increases as the pH of the solution increases. This can

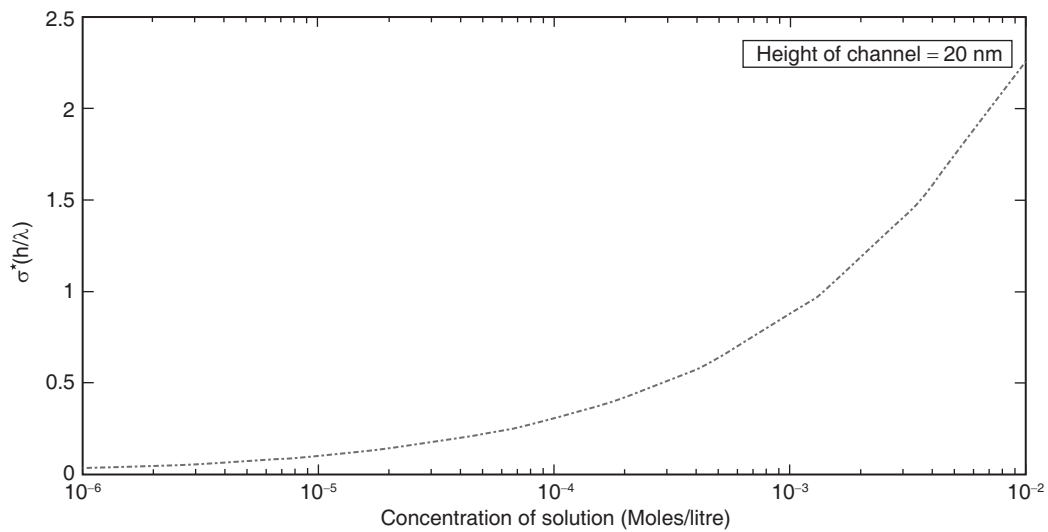


Figure 4. The dependence of surface charge density on the bulk salt concentration of solution for the following input parameters:  $pK=7.5$ ,  $C=2.9$  F/m<sup>2</sup>,  $h = 20$  nm,  $\Gamma = 8/\text{nm}^2$ ,  $pH = 7$

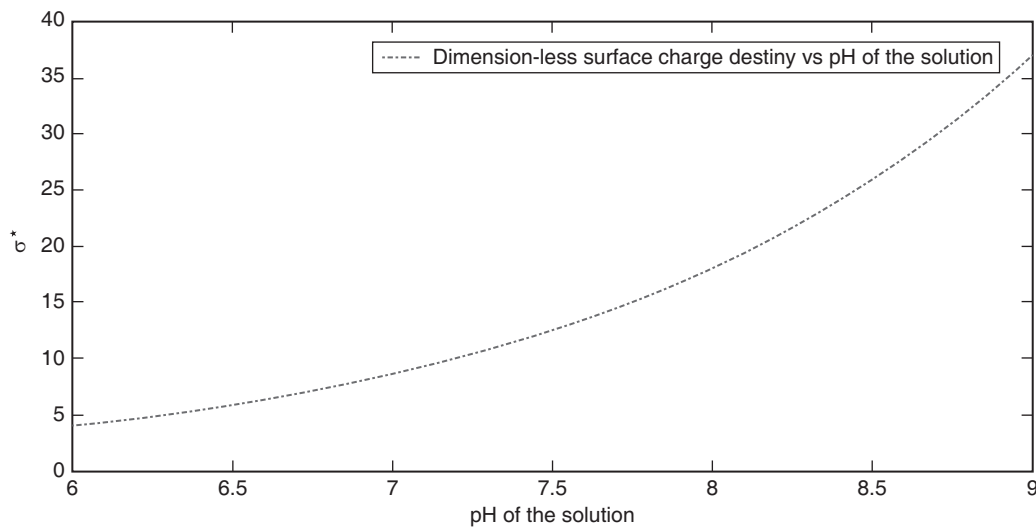


Figure 5. The dependence of surface charge density on pH of solution for the following input parameters:  $pK=7.5$ ,  $C=2.9$  F/m<sup>2</sup>,  $h = 100$  nm,  $\Gamma = 8/\text{nm}^2$ ,  $n_\infty = 0.1\text{mM}$

be explained as for a higher pH value the availability of the H<sup>+</sup> ion in the solution is less which leads to more dissociation of the silica surface (according to the law of mass action). Thus more ions (for the same bulk ionic concentration) are required to counterbalance this charge, which is achieved with a higher electric potential energy level for each ion; therefore, a larger zeta potential results.

In the Stern layer model, the compact layer takes the form of a parallel plate capacitor with opposite charges lining up on the surface and on the Stern plane. The capacitance (per unit area) of such a system is known as “Stern Layer Capacitance”.

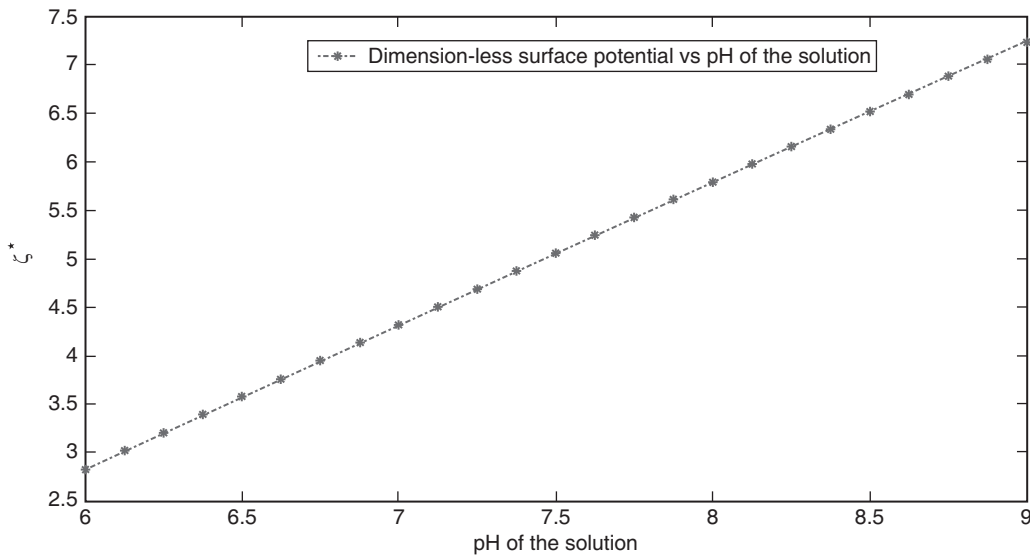


Figure 6. The dependence of surface potential on pH of solution for the following input parameters:  $pK=7.5$ ,  $C=2.9 \text{ F/m}^2$ ,  $h = 100 \text{ nm}$ ,  $\Gamma = 8/\text{nm}^2$ ,  $n_\infty = 0.1 \text{ mM}$

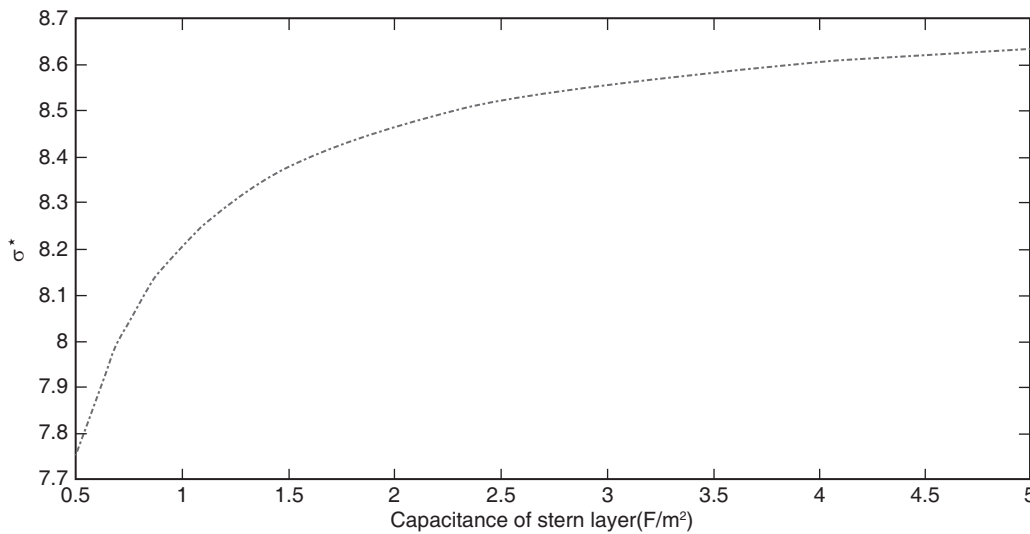


Figure 7. The dependence of surface charge density on the Stern Layer capacitance for following input parameters:  $pK=7.5$ ,  $pH = 7$ ,  $h = 100 \text{ nm}$ ;  $\Gamma = 8/\text{nm}^2$ ,  $n_\infty = 0.1 \text{ mM}$

Figure 7 shows the variation of dimensionless surface charge density ( $\sigma^*$ ) as a function of capacitance of the Stern layer. The range of capacitance values has been chosen to be within the order of magnitudes reported in the literature [9], [16]. It can be observed from the Figure 7 that  $\sigma^*$  increases as the capacitance of Stern layer increases. This behaviour can be understood as follows. If the capacitance of Stern layer is higher, the Stern layer will contribute (by the definition of capacitance) to a lower potential rise from that prevailing at the edge of the diffuse layer (assuming the same charge density); correspondingly, the availability of the  $\text{H}^+$  ions on the surface will become lower, which will lead to a larger degree of dissociation of the silica surface leading to a larger surface charge density.

However, it could be argued that the resultant higher surface charge density could, in turn, mitigate the effect of the increase in Stern layer capacitance by contributing two counteracting tendencies that can *by themselves* increase the  $H^+$  concentration on the charged surface, namely one which increases the potential rise that occurs in Stern layer and the second, which increases the potential at the edge of the diffuse layer (zeta potential). These effects were found not to change the qualitative behaviour of the numerical results indicating that the counteracting effects are less significant than the primary mechanism discussed above.

It can be noted that a saturation in the effect of increasing capacitance is observed in the surface charge density. This is expected because, the limiting case of a Stern layer of infinite capacitance should not cause *any* change in potential across the Stern layer; this corresponds to a diffuse model which neglects the Stern layer altogether. So, the saturation is expected from the fact that larger the capacitance, less significant is the role of Stern layer.

Figure 8 shows the effect of Stern layer capacitance on the zeta potential. The Stern-layer-capacitance dependence of the zeta potential follows a qualitative behaviour similar to the surface charge; *i.e.* the zeta potential increases as the capacitance increases. This is expected, since more net charge in the solution are required to counterbalance an increased surface charge, which can be achieved by attracting more counterions (and repelling co-ions) through a larger surface potential.

The models of EDL developed in this study can also be applied to dynamic situations *i.e.* the study of electrokinetic phenomena provided that such phenomena do not rearrange the layering of ions normal to the nanochannel to a significant degree[30]. For example, in terms of quantities developed in this study the electrical conductance ( $G$ ) [31],[6] of a nanochannel array of  $\hat{N}$  parallel channels each of width  $w$ , length  $L$  and height  $h$  with  $w, L \gg h$  using a symmetric binary 1:1 electrolyte salt with bulk (reservoir) concentration  $n_\infty$  as the conductive fluid can be expressed in the form

$$G = \frac{2\hat{N}wh}{L} n_\infty \left[ \left\{ b_+ \langle \exp(-\phi^*) \rangle + b_- \langle \exp(\phi^*) \rangle \right\} e + \frac{2\epsilon kT}{\mu} \left\langle \left( \frac{d\phi^*}{dy^*} \right)^2 \right\rangle \right] \quad (16)$$

Here,  $\epsilon, \mu$  are the permittivity and viscosity of the electrolyte solution,  $b^+/b^-$  are the mobilities of the co-ion and counter-ion, respectively. In eqn. (16), the first term inside the straight brackets signifies the contribution to conductivity from electromigration of ions and the second term signifies

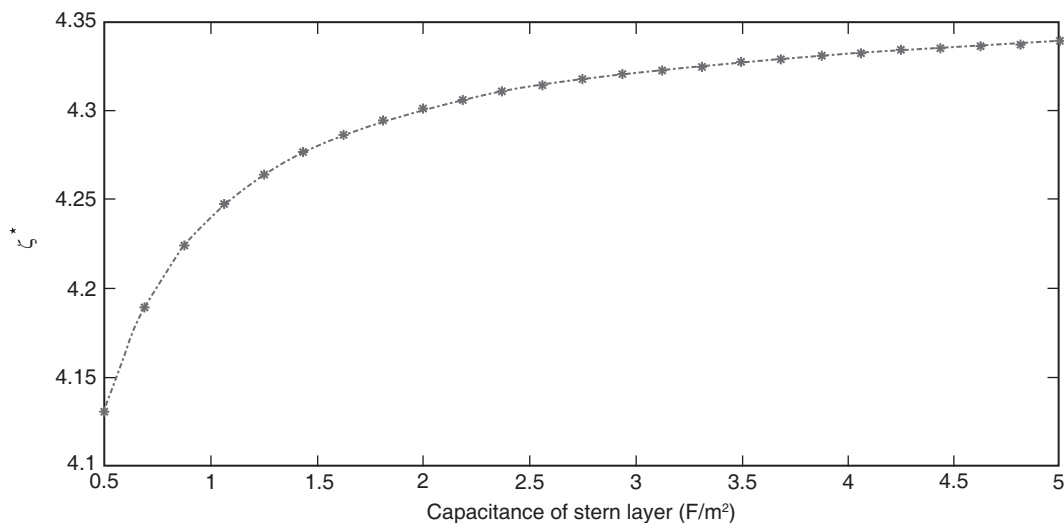


Figure 8. The dependence of surface potential on the stern layer capacitance for following input parameters:  $pK=7.5$ ,  $pH = 7$ ,  $h = 100$  nm;  $\Gamma = 8/\text{nm}^2$ ,  $n_\infty = 0.1\text{mM}$

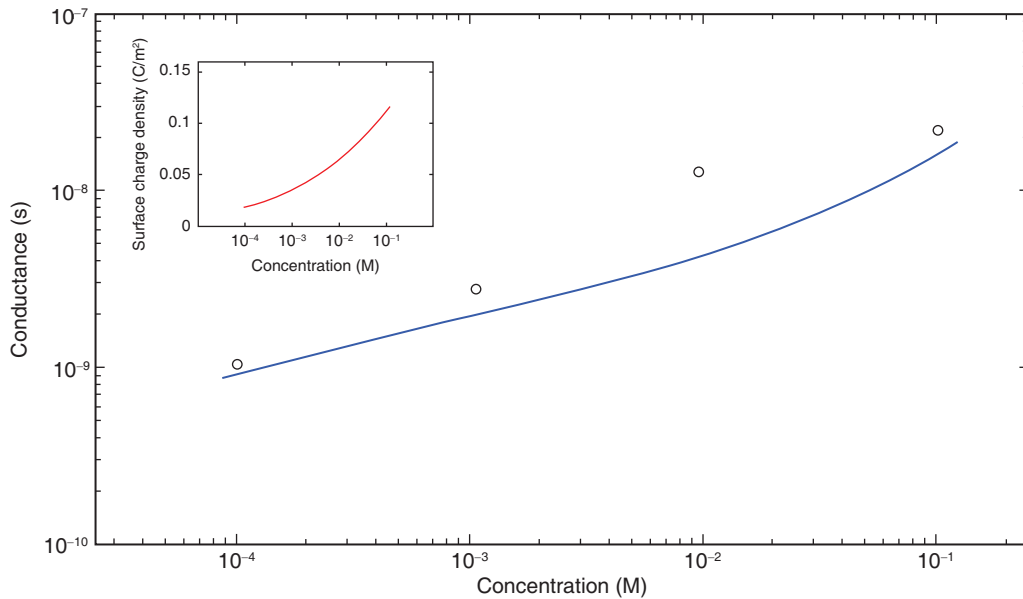


Figure 9. Electrical conductance of nanochannel as a function of the reservoir solution molarity. The input parameters to the model are  $pK = 7.5$ ,  $h = 15$  nm,  $pH = 7$  and  $C = 2.9F/m^2$ . The symbols denote experimental data from [7] and the solid lines are theoretical results. The inset shows the theoretically calculated variation of surface charge density with the molarity of the reservoir solution.

the contribution from transport of net charges by electro-osmotic flow. The angular brackets in eqn. (16) indicate averaging across the channel; the integrand of the second term is evaluated using eqn. (9) and the required integrations are performed using Simpson's rule on a dimensionless grid of spacing  $2.5 \times 10^{-3}$ . The conductance as a function of bulk concentration under an experimental condition ( $h = 15$  nm,  $w = 1$   $\mu$ m,  $L = 120$   $\mu$ m,  $\hat{N} = 30$ ,  $b^+ = 7.91 \times 10^{-8}$  m<sup>2</sup>/s-V,  $b^- = 7.62 \times 10^{-8}$  m<sup>2</sup>/s-V and properties of water at 25°C) observed in [7] (*cf.* electronic supplementary information for this article) has been calculated with the expression in eqn. (16) and compared with the experimental results from the study in Figure 9. The input parameters to the model in this work are  $pK = 5.8$ [9],  $pH = 7$ ,  $C = 2.9F/m^2$ [16]. The resultant surface charge density varies over more than an order of magnitude as shown on the inset to this figure. Karnik et al. [7] has used a model with constant surface charge density instead, which could not represent the measurements in moderately dilute solutions shown in the figure as accurately as in Figure 9; conversely, in very dilute solution the constant surface charge density model is a more accurate representation of experimental observations, as was evident from the aforesaid study as well as another literature study on the fluidic conductance of nanochannels [6].

## 5. CONCLUSIONS

The electric potential distributions studied in this work characterize the ionic distributions in nanochannels, where the characteristic thickness of the EDL is comparable to the cross-channel dimension. The Poisson-Boltzmann equation has been solved in un-linearized form, so that the results are applicable to situation where the electrostatic potential energy of an ion is comparable to or larger than its thermal energy. Both the formation of surface charge and ionic redistribution in the EDL have been considered. Further, both the compact and diffuse parts of the EDL are considered in this work; however, the former is considered only in association with a model of charge accumulation on the surface.

The effects of solution pH, composition, channel geometry and Stern layer as observed in this study can be summarised as follows:

1. The surface charge density decreases and zeta potential increases with increasing pH of the solution.
2. The surface charge density decreases on reducing the channel size, while the zeta potential increases.
3. Both the zeta potential and the surface charge density decreases on reducing the Stern layer capacitance.

While the electrostatic model developed in the current work can be directly utilized to study the interaction forces between surfaces ([32],[33]) the results presented here are also useful for understanding of certain dynamical problems, such as the effect of applied pressure and voltage differentials on fluid flow and current conduction in nanochannels, as relevant to surface characterization [34], bio-separations [35] employing fluid flow through nanochannels (either electro-osmotic or pressure-driven) emerging nanofluidic technologies based on current -voltage and current-pressure characteristics of nanochannels such as fluidic diodes [7] and electrokinetic generators [36]. This is illustrated by the reasonably accurate representation (Figure 9) of the conductance data in [7] by the surface ionization model developed in this study.

Future studies based on the current work can investigate the following aspects:

1. Generalization of the surface ionization model to take into account the adsorption of metal cations
2. Generalization of all the electrostatic models to arbitrary ionic composition of the electrolytes
3. Generalization of the electrostatic models to more complicated geometries
4. Study of electrokinetic phenomena in nanochannels.

For more realistic representation of nano-confinement, it will also be useful to take into account finite-ion-size effects and field-dependent permittivity of water molecules near the silica surface, a simple way to model these effects are through a modified Poisson-Boltzmann equation approach, as discussed in [37], [38] and [39].

As mentioned in point (1) on the list above, a more accurate representation of the pH and salt concentration dependence of zeta potential (whether in microchannels or nanochannels) can be achieved by considering salt cation adsorption on the silica surface. However, this also necessitates a three-layer formalism for the EDL and addition of several parameters to the model that are difficult to measure [11], [9]. After these adjustments, the comparison with microchannel experimental data [9], [12] on zeta potential would be meaningful. It can be noted however, that unlike in microchannels, in nanochannels the zeta potential, itself, have to be ascribed inferred values assuming a certain model for the EDL such as in the current work [21], [34]; future studies can also to be undertaken on the aforementioned problem.

#### ACKNOWLEDGEMENTS

Financial assistance from the SERB division, Department of Science and Technology, India (sanction letter no. SB/FTP/ETA-142/2012) is acknowledged.

#### REFERENCES

- [1] H. Lyklema, *Fundamentals of interface and colloid science Volume II*: Academic press, 1995, vol. Volume II.
- [2] I. Langmuir, "The role of attractive and repulsive forces in the formation of tactoids, thixotropic gels, protein crystals and coacervates.," *The Journal of Chemical Physics*, vol. 6, p. 873, 1938.
- [3] A. J. Corkill and L. Rosenhead, "Distribution of charge and potential in an electrolyte bounded by two plane infinite parallel plates.," *Proceedings of the Royal Society of London. Series A. Mathematical and Physical Sciences*, vol. 172(950), pp. 410–431, 1939.
- [4] D. Burgreen and F. R. Nakache, "Electrokinetic flow in ultrafine capillary slits," *The Journal of Physical Chemistry*, vol. 68, no. 5, pp. 1084–1091, 1964.
- [5] D. Gillespie and S. Pennathur, "Separation of Ions in Nanofluidic Channels with Combined Pressure-Driven and Electro-Osmotic Flow," *Analytical chemistry*, vol. 85, no. 5, pp. 2991–2998, 2013.

- [6] D. Stein, M. Kruthof, and C. Dekker, "Surface-charge-governed ion transport in nanofluidic channels.," *Physical Review Letters*, vol. 93(3), p. 035901, 2004.
- [7] R. Karnik, R. Fan, M., Li D. and Yang, P. Yue, and A. Majumdar, "Electrostatic control of ions and molecules in nanofluidic transistors.," *Nano letters*, vol. 5(5), pp. 943–948, 2005.
- [8] T. W. Healy and L. R. White, "Ionizable surface group models of aqueous interfaces," *Advances in Colloid and Interface Science*, vol. 9, no. 4, pp. 303–345, 1978.
- [9] P. J. Scales, F. Grieser, T. W. Healy, L. R. White, and D. Y. Chan, "Electrokinetics of the silica-solution interface: a flat plate streaming potential study," *Langmuir*, vol. 8, no. 3, 965–974 1992.
- [10] M. Mammen, J. D Carbeck, E. E. Simanek, and G. M. & Whitesides, "Treating Electrostatic Shielding at the Surface of Silica as Discrete Siloxide-Cation Interactions," *Journal of the American Chemical Society*, vol. 119, no. 15, pp. 3469–3476, 1997.
- [11] A. Revil, P. A. Pezard, and P. W. J. Glover, "Streaming potential in porous media: 1. Theory of the zeta potential.," *Journal of Geophysical Research: Solid Earth (1978–2012)*, vol. 104, no. B9, pp. 20021–20031, 1999.
- [12] B. J. Kirby and E. F. Hasselbrink, "Zeta potential of microfluidic substrates: 1. Theory, experimental techniques, and effects on separations.," *Electrophoresis*, vol. 25(2), pp. 187–202, 2004.
- [13] R. B. Schoch, J. Han and P. Renaud, "Transport phenomena in nanofluidics.," *Reviews of Modern Physics*, vol. 80(3), p. 839, 2008.
- [14] E. Yariv, "Electro-osmotic flow near a surface charge discontinuity," *Journal of Fluid Mechanics*, vol. 521, pp. 181–189, 2004.
- [15] P. Dutta and A. Beskok, "Analytical solution of combined electroosmotic/pressure driven flows in two-dimensional straight channels: finite Debye layer effects," *Analytical Chemistry*, vol. 73, no. 9, pp. 1979–1986, 2001.
- [16] S. H. Behrens and D. G. Grier, "The charge of glass and silica surfaces.," *Journal of chemical physics*, vol. 115(14), pp. 6716–6721, 2001.
- [17] R. Qiao and N. R. Aluru, "Ion concentrations and velocity profiles in nanochannel electroosmotic flows.," *The Journal of chemical physics*, vol. 118, p. 4692, 2003.
- [18] Z. Zheng, D. J. Hansford, and A. T. Conlisk, "Effect of multivalent ions on electroosmotic flow in micro? and nanochannels.," *Electrophoresis*, vol. 24(17), pp. 3006–3017, 2003.
- [19] X. Xuan and D. Li, "Electrokinetic transport of charged solutes in micro?and nanochannels: The influence of transverse electromigration.," *Electrophoresis*, vol. 27(24), pp. 5020–5031, 2006.
- [20] E. Papirer (Ed.). *Adsorption on silica surfaces*. CRC Press, 2000.
- [21] Siddhartha Das, Arnab Guha, and Sushanta K Mitra, "Exploring new scaling regimes for streaming potential and electroviscous effects in a nanocapillary with overlapping Electric Double Layers," *Analytica Chimica Acta*, 2013.
- [22] Fabio Baldessari and Juan Santiago, "Electrokinetics in nanochannels: Part I. Electric double layer overlap and channel-to-well equilibrium," *Journal of colloid and interface science*, vol. 325, no. 2, pp. 526–538, 2008.
- [23] S. Datta and A. T. Conlisk, "Role of multivalent ions and electrical double layer overlap in electroosmotic nanoflows.," , In Proceedings of the 47th AIAA Aerospace Sciences Meeting., January 2009.
- [24] S. Talapatra and S. Chakraborty, "Double layer overlap in ac electroosmosis.," *European Journal of Mechanics-B/Fluids*, vol. 27(3), pp. 297–308, 2008.
- [25] W. Qu and D. Li, "A model for overlapped EDL fields," *Journal of Colloid and Interface Science*, vol. 224(2), pp. 397–407, 2000.
- [26] H. S. Kwak and E. F. Hasselbrink Jr, "Timescales for relaxation to Boltzmann equilibrium in nanopores.," *Journal of colloid and interface science*, vol. 284(2), pp. 753–758, 2005.

- [27] C. L. Rice and R. Whitehead, "Electrokinetic flow in a narrow cylindrical capillary," *The Journal of Physical Chemistry*, 1965.
- [28] Pankaj Asija, "Modelling electrostatics in nanochannels," IIT Delhi, M. Tech. Thesis 2013.
- [29] M Abramowitz and A Stegun, *Handbook of Mathematical Functions*, 9th ed.: Dover Publications, 1972.
- [30] S. Ghosal, "Electrokinetic flow and dispersion in capillary electrophoresis.," *Annu. Rev. Fluid Mech*, vol. 38, pp. 309–338, 2006.
- [31] S. Levine, J. R. Marriott, and K. Robinson, "Theory of electrokinetic flow in a narrow parallel-plate channel.," *J. Chem. Soc., Faraday Trans. 2*, vol. 71, pp. 1–11, 1975.
- [32] J. N. Israelachvili, *Intermolecular and surface forces: revised third edition*, 3rd ed.: Academic press., 2011.
- [33] E. J. W. Verwey and J. T. G. Overbeek, *Theory of the stability of lyophobic colloids.:* Courier Dover Publications., 1999.
- [34] S. Datta, A. T. Conlisk, D. M. Kanani, A. L. Zydney, W. H. Fissell, and S. Roy, "Characterizing the surface charge of synthetic nanomembranes by the streaming potential method.," *Journal of colloid and interface science*, vol. 348(1), pp. 85–95, 2010.
- [35] S. Pennathur and J. G. Santiago, "Electrokinetic transport in nanochannels. 2. Experiments.," *Analytical chemistry*, vol. 77(21), pp. 6782–6789, 2005.
- [36] F. H. Van der Heyden, D. Stein, and C. Dekker, "Streaming currents in a single nanofluidic channel.," *Physical review letters*, vol. 95(11), p. 116104, 2005.
- [37] Aditya Bandopadhyay and Suman Chakraborty, "Steric-effect induced alterations in streaming potential and energy transfer efficiency of non-Newtonian fluids in narrow confinements," *Langmuir*, vol. 27, no. 19, pp. 12243–12252, 2011.
- [38] Itamar Borukhov, David Andelman, and Henri Orland, "Steric effects in electrolytes: a modified Poisson-Boltzmann equation," *Physical review letters*, vol. 79, no. 3, p. 435, 1997.
- [39] Siddhartha Das, Suman Chakraborty, and Sushanta K Mitra, "Redefining electrical double layer thickness in narrow confinements: Effect of solvent polarization," *Physical Review E*, vol. 85, no. 5, p. 051508, 2012.